PERGAMON

Renewable Energy 26 (2002) 309–323

RENEWABLE ENERGY

www.elsevier.com/locate/renene

Technical note

Numerical analysis of two dimensional parallel flow flat-plate solar collector

H. Kazeminejad *

Gamma Irradiation Center, Atomic Energy Organization of Iran, P.O. Box 11365-8486, Tehran, I.R. Iran

Received 1 May 2001; accepted 14 May 2001

Abstract

Temperature distribution over the absorber plate of a parallel flow flat-plate solar collector is analyzed with one- and two-dimensional steady-state conduction equations with heat generations. The governing differential equations with boundary conditions are solved numerically using a control volume-based finite difference scheme. Comparisons of one- and two-dimensional results showed that the isotherms and performance curve, stated in terms of an effectiveness/number-of-transfer-unit relationship, for one-dimensional analysis slightly deviate from that of two-dimensional analysis, particularly under low mass flow rate conditions. In addition, collector efficiency as a function of operating point is computed and presented graphically for different collector configuration and various operating conditions. For general engineering purposes, these performance curves may be used for efficient and optimum design of liquid flat-plate solar collectors.

1. Introduction

The parallel flow flat-plate solar collector is commonly used today for the collection of low temperature solar thermal energy. Conventional analysis and design of this kind of collectors is based on a one-dimensional conduction equation formulation [1]. The analysis has been substantially assisted by the derivation of plate-fin efficiency factors. The factors relate the design and operating conditions of the collector in a systematic manner that facilitates prediction of heat collection rates at the design stage. The one-dimensional analysis offers a desired accuracy required in a routine analysis even though a two-dimensional temperature distribution exists over

* Corresponding author. Tel.: +98-21-8004065; fax: +98-21-8009054.

0960-1481/02/$ - see front matter
PII: S0960-1481(01)00121-5

Nomenclature

A_c	collector area [m^2]
C_c	collector circumference [m]
C_f	fluid heat capacity rate, $C_f=mC_p$ [W/K]
C_p	fluid specific heat [J/kg·K]
Gr_m	arithmetic mean Grashof number, $Gr_m=\Delta T d_i g/v^2$
Gz_m	arithmetic mean Graetz number, $Gz_m=mC_p/k_fL$
I	Flux incident on the top cover of the collector [W/m^2]
L	length of absorber in the flow direction [m]
L^*	Characteristic dimension, $L^*=4A_c/C_c$ [m]
M	number of glass covers
N	collector number of transfer units, $N=U_LWL/C_f$
Nu_m	arithmetic mean Nusselt number, $N_m=hd_i/k_f$
Pr_m	arithmetic mean Prandtl number, $Pr_m=\mu C_p/k_f$
Re	Reynolds number, $Re=(V_\infty L^*/v)$
S	solar irradiance absorbed [w/m^2]
T	plate temperature [°C]
T_f	fluid temperature function [°C]
T_{fi}	fluid inlet temperature [°C]
T_{fo}	fluid outlet temperature [°C]
T_{pm}	plate mean temperature [°C]
T_{ps}	plate stagnation temperature [°C]
T_∞	ambient temperature [°C]
U_l	overall heat loss coefficient [W/m^2·K]
U_t	top heat loss coefficient [W/m^2·K]
V_∞	wind velocity [m/s]
W	half-pitch distance between flow tubes [m]
X_{cas}	casing thickness [m]
X_{ins}	insulation thickness [m]
d_i	tube internal diameter [m]
d_o	tube external diameter [m]
h_f	convection heat transfer coefficient, tube to fluid [W/m^2·K]
h_{fe}	equivalent convection heat transfer coefficient [W/m^2·K]
h_s	convection heat transfer coefficient at the plate top and bottom [W/m^2·K]
h_w	convection heat transfer coefficient at the glass cover [W/m^2·K]
k_{cas}	casing thermal conductivity [W/m·K]
k_f	plate thermal conductivity [W/m·K]
k_{ins}	insulation thermal conductivity [W/m·K]
k_p	plate thermal conductivity [W/m·K]
m	mass flow rate [kg/s]
x,y	coordinates

β	altitude angle
δ_p	plate thickness [m]
ε	absorber effectiveness, $\varepsilon=(T_{fo}-T_{fi})/(T_{ps}-T_{fi})$
ε_g	glass cover emissivity
ε_p	absorber plate emissivity
μ_b	fluid dynamic viscosity at bulk temperature [kg/s·m]
μ_w	fluid dynamic viscosity at wall temperature [kg/s·m]
ν	fluid kinematics viscosity [m^2/s]
σ	Stefan–Boltzman constant

the absorber plate of the collector. Therefore, for more accurate analysis at low mass flow rates, a two-dimensional temperature distribution must be considered.

Various investigators have used two dimensional conduction equations in their analysis with different boundary conditions. Rao et al. [2] proposed a two-dimensional model for the absorber plate conduction to compute the fluid temperature rise. Lund [3] used a two-dimensional model for the transfer of heat in flat plate solar collector absorbers with adiabatic boundary conditions at the upper and lower edges of the collector. He solved approximately the governing partial differential equations analytically in terms of perturbation series. In similarity to heat exchanger theory, collector performance was stated in terms of absorber thermal effectiveness and number of transfer unit relationship. Nag et al. [4] used the two-dimensional model proposed by Lund, but with convection boundary condition at the upper and lower edge of the absorber plate. They solved the governing equations using finite element method. Without comparison with the one-dimensional analysis, they concluded that the isotherms deviate from a one-dimensional pattern for a high flow rate to a predominantly two-dimensional distribution for a low mass flow rate. Although all these investigators have used a two-dimensional model for the conduction equation, they have not compared their results with those obtained using the conventional one-dimensional analysis. Here, the one- and two-dimensional conduction equation with different boundary conditions were solved using an efficient finite volume method. Results are presented in terms of absorber thermal effectiveness and number of transfer units and compared with those obtained using the conventional analysis. Also, the performance of a liquid flat-plate collector for different design, operational, meteorological and environmental parameters was investigated.

2. Theoretical model

The collector whose coordinate and geometric parameters are illustrated in Fig. 1 is considered. By assuming that the heat loss from the collector occurs, approximately, to the one ambient temperature, a heat balance on a differential volume of the absorber plate yields the following two-dimensional, steady state conduction equation.

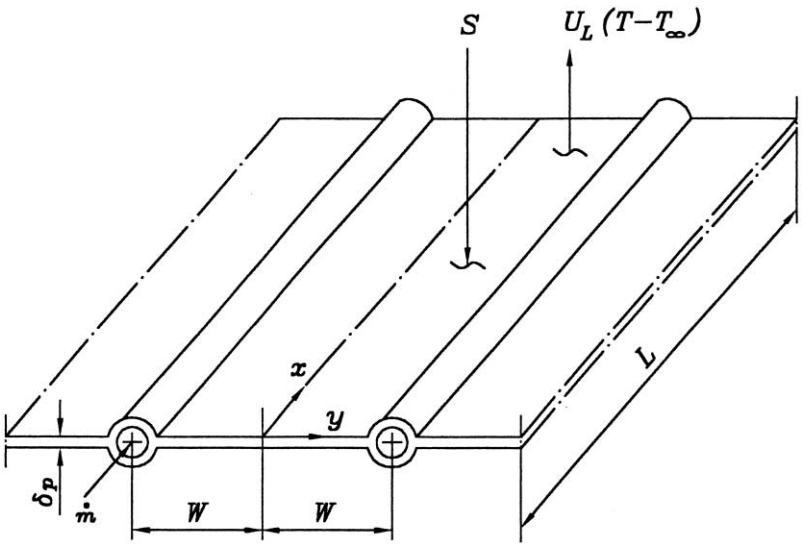

Fig. 1. Typical collector absorber plate and coordinate system.

$$\frac{\partial^2 T}{\partial x^2}+\frac{\partial^2 T}{\partial y^2}+\frac{[S-U_l(T-T_\infty)]}{k_p\delta_p}=0 \text{ in } 0<x<W,\ 0<y<L \tag{1}$$

with boundary conditions

$$\frac{\partial T}{\partial x}+\frac{h_{fe}[T-T_f(y)]}{k_p}=0 \text{ on } x=W,\ 0\le y\le L \tag{2}$$

$$\frac{\partial T}{\partial y}+\frac{h_s(T-T_\infty)}{k_p}=0 \text{ on } 0\le x\le W,\ y=L \tag{3}$$

$$\frac{\partial T}{\partial x}=0.0 \text{ on } x=0,0\le y\le L \tag{4}$$

$$\frac{\partial T}{\partial y}-\frac{h_s(T-T_\infty)}{k_p}=0 \text{ on } 0\le x\le W,\ y=0 \tag{5}$$

where $T(x,y)$ represents the plate temperature, k_p is plate thermal conductivity, $T_f(y)$ is fluid temperature and T_∞ is ambient temperature. S is the incident solar flux absorbed in the absorber plate, U_l the overall heat loss coefficient and δ_p is the absorber plate thickness. The overall heat loss coefficient, U_l, is defined by the following equation:

$$U_l=U_t+U_b \tag{6}$$

where U_t and U_b are top heat loss coefficient and bottom heat loss coefficient, respectively. Based on calculations for a large number of cases covering the entire range of conditions normally expected for flat plate collectors, Klein [5] has

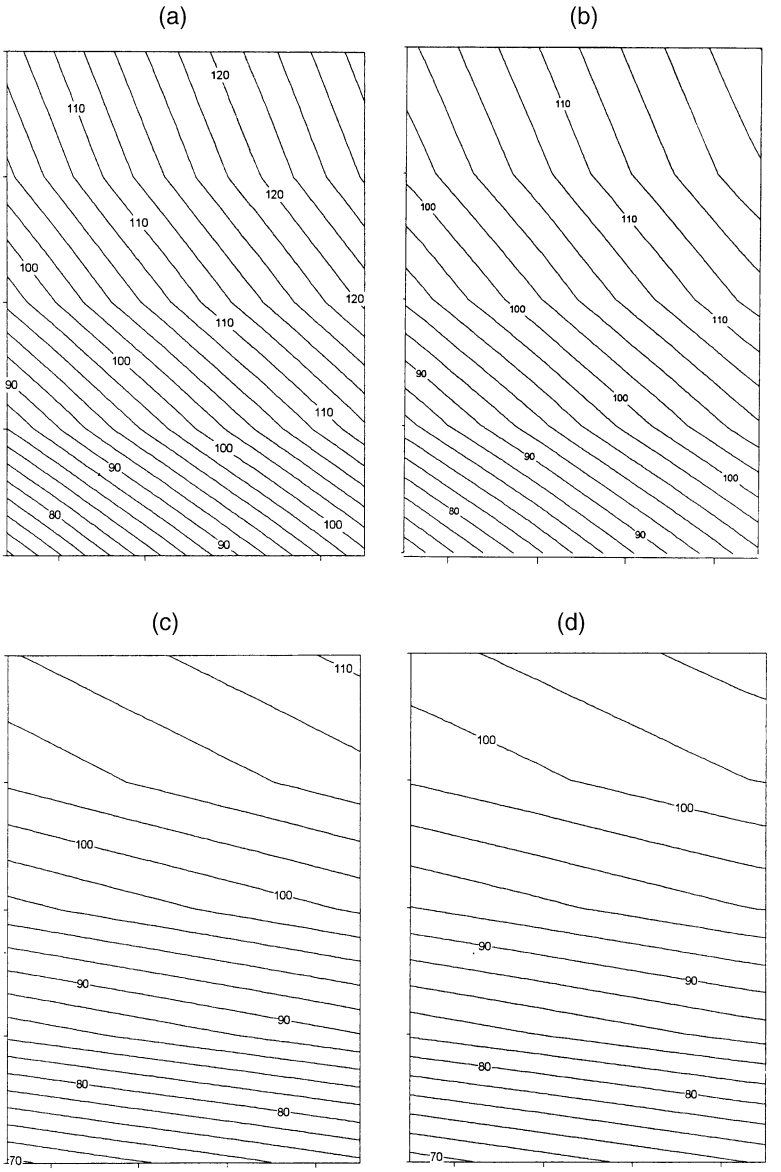

Fig. 2. Isotherm pattern over the absorber plate: (a) 1-D analysis, low mass flow rate, m=0.002 kg/s; (b) 2-D analysis, low mass flow rate, m=0.002 kg/s; (c) 1-D analysis, high mass flow rate, m=0.01 kg/s; (d) 2-D analysis, high mass flow rate, m=0.01 kg/s.

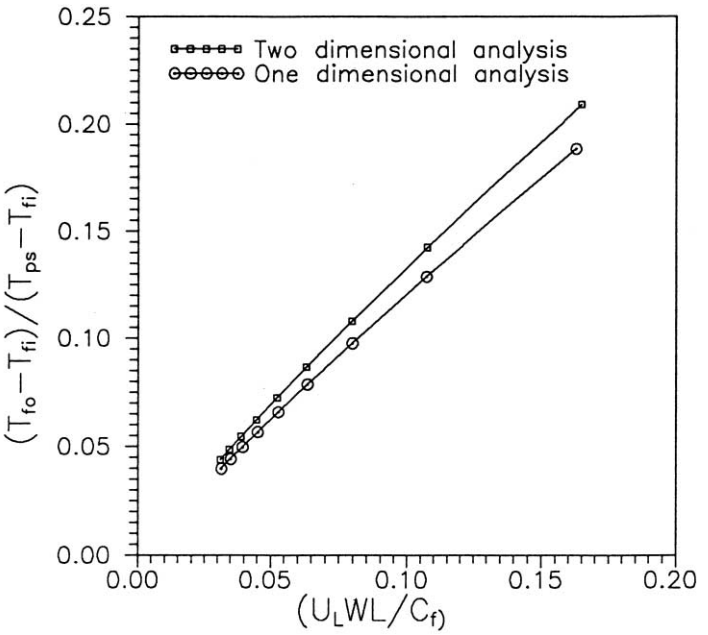

Fig. 3. Comparisons of effectiveness vs number of transfer units for one- and two-dimensional analysis.

developed the following convenient equation for calculating the top heat loss coefficient, U_t:

$$U_t=\left[\frac{M}{\left(\frac{C}{T_{pm}}\right)\left(\frac{T_{pm}-T_\infty}{M+f}\right)^{0.33}}+\frac{1}{h_w}\right]^{-1}+ \tag{7}$$

$$\left[\frac{\sigma(T_{pm}^2+T_\infty^2)(T_{pm}+T_\infty)}{\frac{1}{\varepsilon_p+0.05M(1-\varepsilon_p)}+\frac{(2M+f-1)}{\varepsilon_g}-M}\right]$$

where

$$f=(1-0.04h_w+0.0005h_w^2)(1+0.091M)$$

$$C=365.9(1-0.00883\beta+0.0001298\beta^2)$$

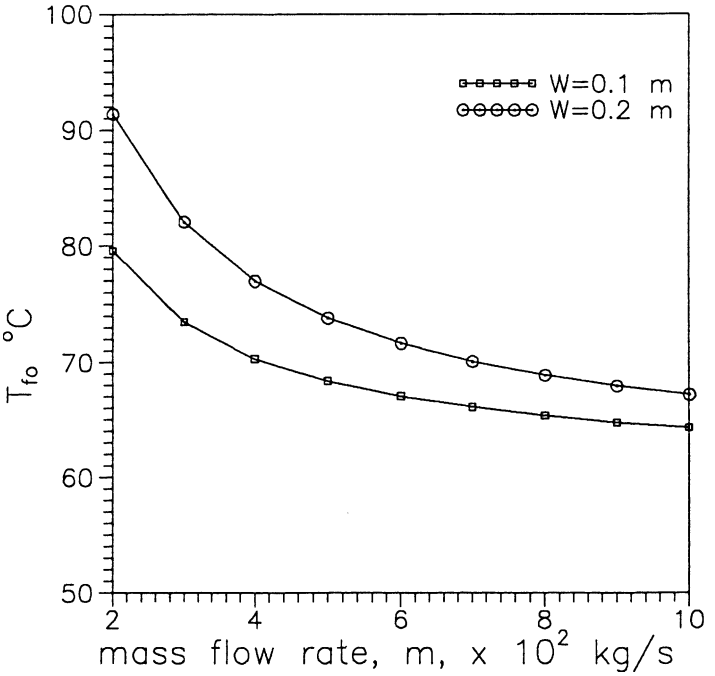

Fig. 4. Effect of tube spacing, w, on fluid outlet temperature, T_{fo}.

M=number of glass covers

While using Eq. (7), T_{pm} and T_∞ are expressed in K, h_w in W/m^2·K, σ in W/m^2·K^4, and β, the collector tilt angle, in degrees. The value of U_t is obtained in W/m^2·K. The range of conditions over which Eq. (7) has been developed, is as follows:

$320 \le T_{pm} \le 420$ K

$260 \le T_\infty \le 310$ K

$0.1 \le \varepsilon_p \le 0.95$

$0 \le V_\infty \le 10$ m/s

$1 \le M \le 3$

$0 \le \beta \le 90°$

Although not explicitly stated, it appears that the values of ε_g and spacing between absorber plate and cover or between covers have been taken to be constant and equal to 0.88 and 2.54 cm, respectively. The convective heat transfer coefficient, h_w, at the top cover is calculated from the following empirical correlation suggested by Sparrow and Tien [6].

$$j=(h_w/\rho C_p V_\infty)Pr^{2/3}=0.86\,Re^{-(1/2)} \tag{8}$$

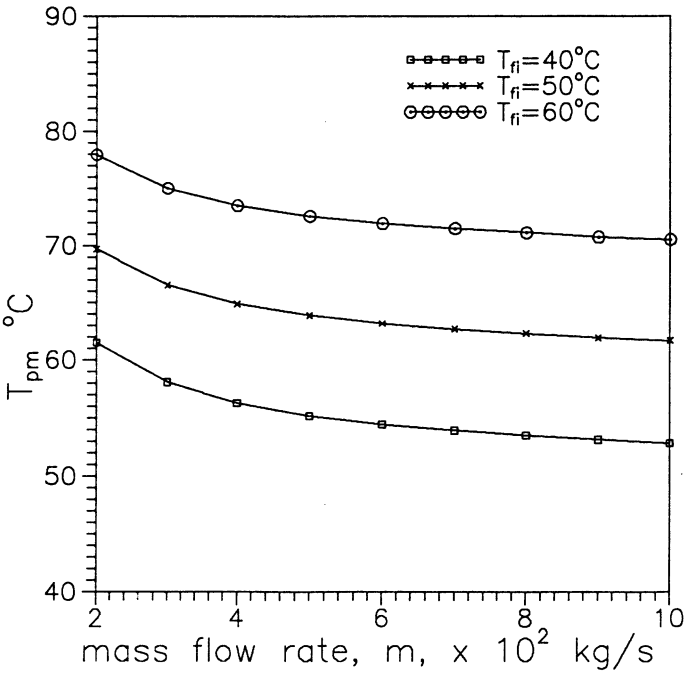

Fig. 5. Effect of fluid inlet temperature, T_{fi}, on plate mean temperature, T_{pm}.

The bottom heat loss coefficient, U_b, tube side effective heat transfer coefficient, h_{fe}, and edge heat transfer coefficient, h_s, are evaluated as follows [4]:

$$U_b=\frac{1}{(X_{ins}/k_{ins})+(X_{cas}/k_{cas})} \tag{9}$$

$$h_{fe}=\left(\frac{1}{\delta_p}\right)\left[\frac{\pi d_i h_f}{2}+\frac{\pi d_o(T-T_\infty)}{4(T-T_f)}-\frac{d_o S}{2(T-T_f)}\right] \tag{10}$$

$$h_s=\frac{1}{(X_{ins}/k_{ins})+(X_{cas}/k_{cas})} \tag{11}$$

where X_{ins} and X_{cas} are thickness of insulation and casing, respectively, k_{ins} and k_{cas} represent conductivities of insulation and casing, respectively. d_i, d_o and h_f stand for the tube inside diameter, tube outside diameter and tube side heat transfer coefficient, respectively.

Film heat transfer coefficients in solar collector tubes at low Reynolds numbers were investigated experimentally by Baker [7]. The investigation was made into the internal, laminar flow, heat transfer characteristics of a tube similar to the type used in tube in-strip solar collector plates. For such a tube it was concluded that, due to significant variation in the circumferential wall temperature, the heat transfer rates

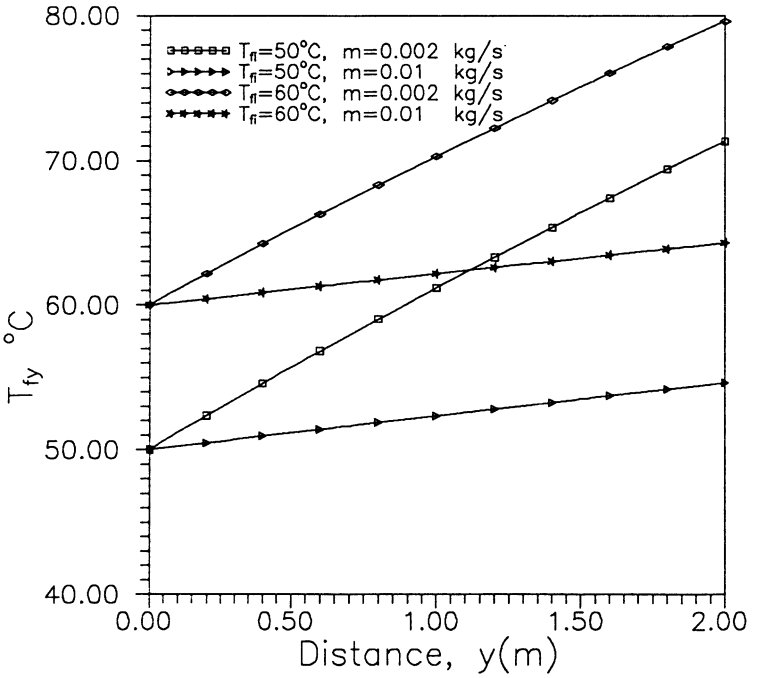

Fig. 6. Variation of fluid temperature, T_f, along the tube for different T_{fi}, and m.

are higher than would be obtained in a tube with uniform wall temperature. Also, the most probable mode of heating water in solar collector tubes is mixed convection and the Oliver's correlations provide a reliable guide for the determination of the film heat transfer coefficient, h_f. Based on experimental work, Oliver [8] have suggested the following correlations.

$$Nu_m = 1.75(\mu_b/\mu_w)^{0.14}[Gz_m + 0.0083(Gr_m Pr_m)^{0.75}]^{1/3} \tag{12}$$

for tubes with L/d_i ratio >70 and

$$Nu_m = 1.75(\mu_b/\mu_w)^{0.14}\left[Gz_m + 0.00056\left(Gr_m Pr_m \frac{L}{D}\right)^{0.70}\right]^{1/3} \tag{13}$$

For tubes with L/d_i ratio <70.

The fluid temperature distribution $T_f(y)$ for inlet temperature, T_{fi}, fluid mass flow rate, m, and specific heat, C_p, is explicitly given as:

$$T_f(y) = T_{fi} + \frac{2}{mC_p}\int_0^y \left[-k_p\delta_p\frac{\partial T}{\partial x} + \frac{d_o S}{2} - \frac{\pi d_o U_l (T - T_\infty)}{4}\right]_{x=W} dy \tag{14}$$

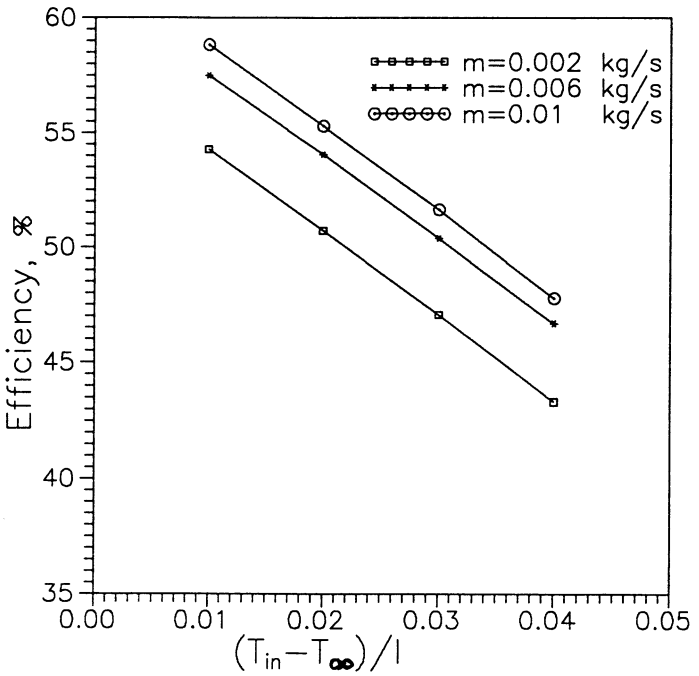

Fig. 7. Effect of mass flow rate, m, on efficiency, λ.

3. Solution

Finite-difference approximations of Eq. (1) were solved numerically in conjunction with the boundary conditions (2)–(5). The numerical scheme was based on the control-volume formulation, Patankar [9], and the tri-diagonal matrix algorithm (TDMA) for solving the system of discretized equations. Since the set of algebraic equations is non-linear in nature, because of the radiative term in U_l, an iterative procedure was used. The local criterion for numerical convergence (the maximum relative difference between two consecutive iterations for any local variable) was 10^{-3}. The rectangular domain x and y was covered with an orthogonal non-uniform grid.

4. Results and discussions

The present parametric study is based on the meteorological data for Bosher (29.98°N) during the month of June. Monthly averaged hourly solar radiation at solar noon is I=703 W/m^2, Daneshyar [10]. Following is a list of other pertinent parameters:

L=2 m, δ_p=1 mm, d_i=10 mm, d_o=11 mm, ε_p=0.17, ε_g=0.88, k_{ins} =0.04 W/m·K, x_{ins}=0.05 m, T_∞=30°C, C_p=4180 J/kg K

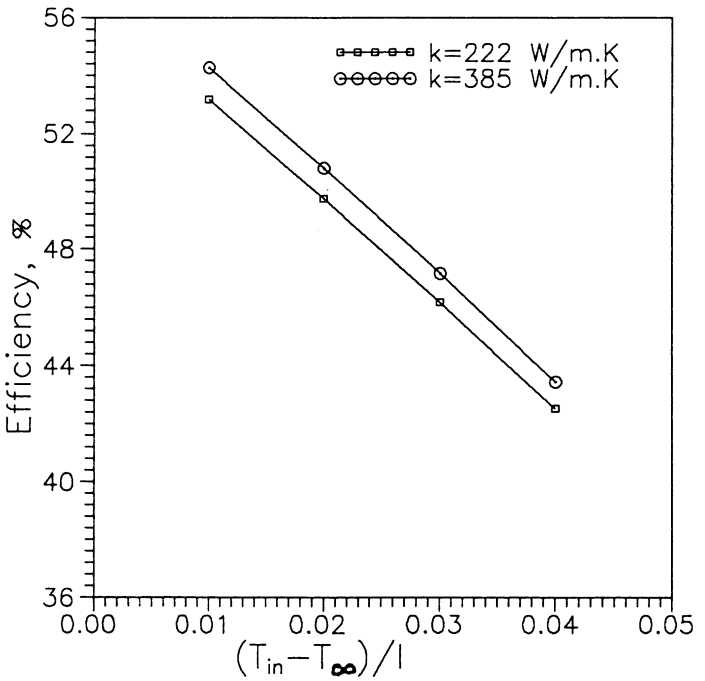

Fig. 8. Effect of plate thermal conductivity, k, on efficiency, λ.

where L is collector length, ε_p is plate emissivity and ε_g is glass cover emissivity.

Figs. 2(a)–(c) demonstrate the isotherm patterns over the absorber plate for different mass flow rates. The isotherms deviate from a more or less one-dimensional pattern for a high flow rate to a predominantly two-dimensional distribution for a low mass flow rate. This indicates that for a low mass flow rate a two-dimensional analysis is desirable.

Fig. 3 shows the variation of absorber effectiveness, with collector number of transfer units for one- and two-dimensional analysis. Effectiveness is seen to increase with increasing the number of transfer units. Also, the difference between the one- and two-dimensional analysis is seen to increase with increasing the number of transfer units, with the two-dimensional analysis predicting higher values than the conventional one-dimensional analysis. It must be noted that at lower values of the number of transfer units or higher mass flow rates, the effectiveness predicted by the one- and two-dimensional analysis are almost the same. This finding confirms that, at higher values of the number of transfer units or lower values of mass flow rates, the two-dimensional analysis must be considered.

Variations of fluid outlet temperature and plate mean temperature for different mass flow rates, inlet water temperatures and tube spacing are shown in Figs. 4 and 5. It can be seen that the fluid outlet temperature and plate mean temperature decrease with an increase in the mass flow rate, whereas increasing the tube spacing or fluid inlet temperature will increase the fluid outlet and plate mean temperature. Also, in

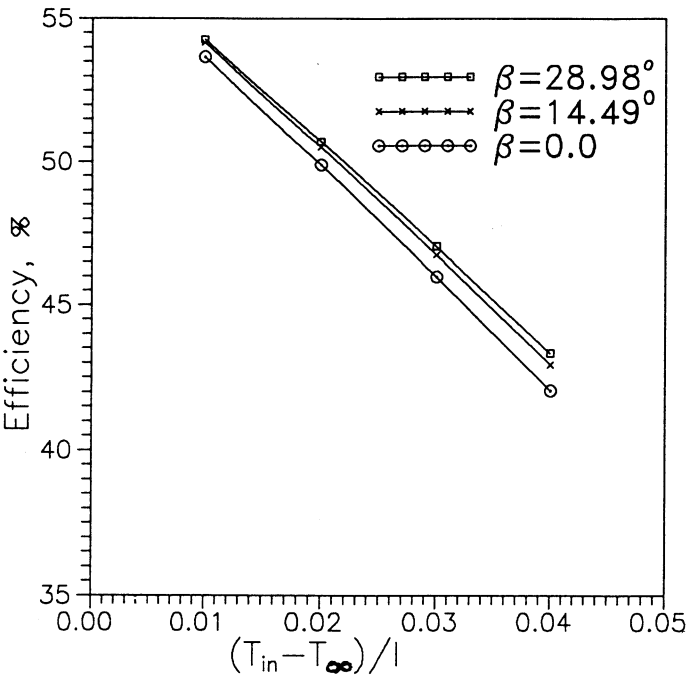

Fig. 9. Effect of tilt angle, β, on efficiency, λ.

collector design, the knowledge of plate mean temperature is required for determination of collector top loss coefficient.

Fig. 6 shows fluid temperature distribution along the tube length for different mass flow rates and different fluid inlet temperatures. A uniform increase of fluid temperature, for different cases shown, suggests that collector length can be increased beyond its present dimension with effective useful energy being delivered from the collector.

Variation of collector efficiency with operating parameter, $(T_{fi}-T_{\infty})/I$, for different mass flow rates is illustrated in Fig. 7. It is seen that the efficiency increases with increasing mass flow rates. This may be explained by the fact that the increase in mass flow rate is accompanied by an increase in the convection heat transfer coefficient to the fluid, thus enhancing the rate of heat transfer to fluid. The increase in mass flow rate will also decrease plate mean temperature, therefore reducing heat loss to the environment. These effects will improve collector efficiency.

Collector efficiency, for two different collector materials (copper and aluminum), and different mass flow rates are shown in Fig. 8. The marginal variation indicates the possibility of using less expensive materials such as aluminum, instead of copper, for collector plates.

Computation of the collector efficiency, for three different tilt angles, β, are illustrated in Fig. 9. It is generally recommended that for year-round use, the optimum tilt angle for maximum efficiency of a flat-plate liquid collector facing south should

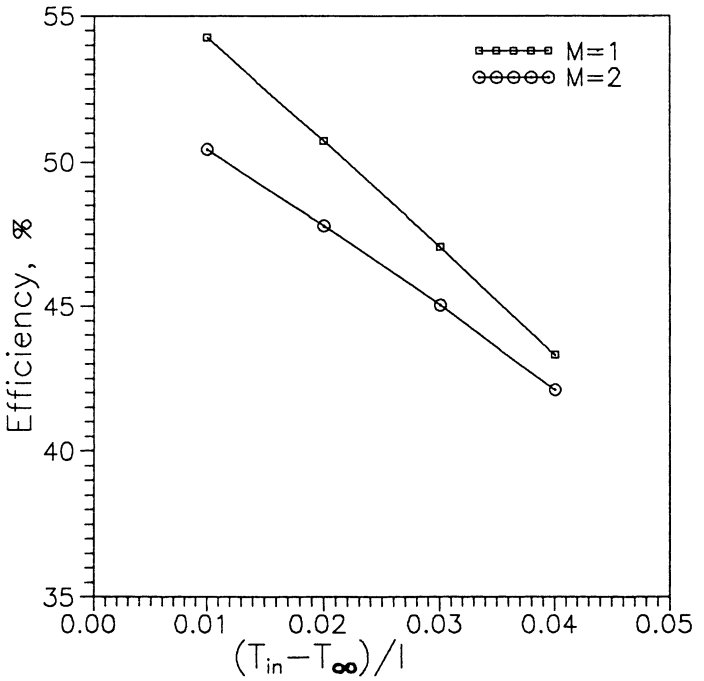

Fig. 10. Effect of number of glass cover, M, on efficiency, λ.

be equal to the latitude angle, i.e. 28.98°. The present results indicate that, for the location of the present study, the appropriate tilt angle for the collector is consistent with the recommended optimum value and also collector efficiency decreases with decreasing the tilt angle.

The number of covers used in a collector is usually one or two. As the number of covers increases, the solar irradiance, S, absorbed by the absorber plate decreases. Also, the addition of more covers causes the value of U_t, and hence the heat loss, to decrease. However, the amount of decrease is not the same in both cases and the efficiency increases. This is not the case with all kinds of collectors. In fact, for the collector under study, Fig. 10, the efficiency is found to be highest with only one glass cover. The effect of tube spacing on collector efficiency is illustrated in Fig. 11. With increasing tube spacing, heat removal rate per unit collector area decreases while the plate mean temperature and loss to the environment increase with a consequential loss of efficiency.

5. Conclusions

The performance of one- and two-dimensional flat-plate liquid collectors was investigated numerically. From the preceding results and discussions it is evident that the conventional one-dimensional method is accurate enough for most engineering

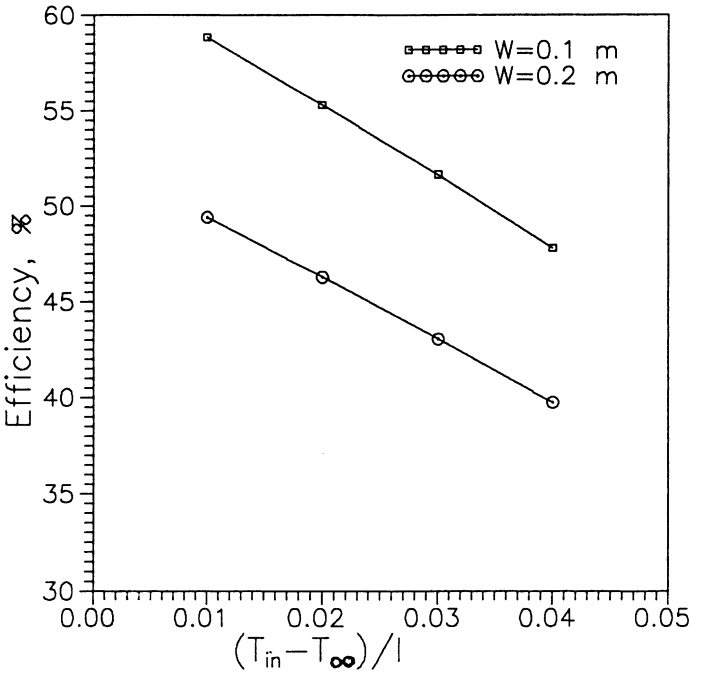

Fig. 11. Effect of tube spacing, w, on efficiency, λ.

purposes. However, for optimum design, a two-dimensional analysis must be considered, especially at lower mass flow rates.

The results also show that a large number of parameters influence the performance of a liquid flat-plate collector. Among the design parameters, operational parameters, meteorological parameters and environmental parameters, the fluid inlet temperature, mass flow rate and tube spacing strongly influence the performance of a flat-plate collector.

References

[1] Sukhatme SP. Solar energy, principles of thermal collection and storage. New Delhi: Tata McGraw-Hill, 1991.
[2] Rao PP. Two-dimensional analysis of a flat plate solar collector. J Energy 1977;1:324.
[3] Lund KO. General thermal analysis of parallel-flow flat-plate solar collector absorbers. Solar Energy 1986;5:443.
[4] Nag A, Misra D, De KE, Bhattacharya A, Saha SK. Parametric study of parallel flow flat plate solar collector using finite element method. In: Numerical Methods in Thermal Problems, Proceedings of the 6th International Conference, Swansea, UK, 1989.
[5] Klein SA. Calculation of flat-plate collector loss coefficient. Solar Energy 1977;17:79.
[6] Sparrow EM, Tien KK. Forced convection heat transfer at an inclined and yawed square plate—Application to solar collector. J Heat Transfer, Trans ASME 1977;99:507.

[7] Baker HL. Film heat transfer coefficients in solar collector tubes at low Reynolds numbers. Solar Energy 1967;11(2):78.
[8] Oliver DR. The effect of natural convection on viscous-flow heat transfer in horizontal tubes. Chem Eng Sci 1962;17:335.
[9] Patankar SV. Numerical heat transfer and fluid flow. New York: Hemisphere Publishing, Taylor and Francis Group, 1980.
[10] Daneshyar M. Solar radiation statistics for Iran. Solar Energy 1978;21:345.